Doppler Radar Fall Activity Detection Using the Wavelet Transform

Bo Yu Su, *Student Member, IEEE*, K. C. Ho, *Fellow, IEEE*, Marilyn J. Rantz, *Member, IEEE*, and Marjorie Skubic, *Senior Member, IEEE*

***Abstract*—We propose in this paper the use of Wavelet transform (WT) to detect human falls using a ceiling mounted Doppler range control radar. The radar senses any motions from falls as well as nonfalls due to the Doppler effect. The WT is very effective in distinguishing the falls from other activities, making it a promising technique for radar fall detection in nonobtrusive inhome elder care applications. The proposed radar fall detector consists of two stages. The prescreen stage uses the coefficients of wavelet decomposition at a given scale to identify the time locations in which fall activities may have occurred. The classification stage extracts the time–frequency content from the wavelet coefficients at many scales to form a feature vector for fall versus nonfall classification. The selection of different wavelet functions is examined to achieve better performance. Experimental results using the data from the laboratory and real inhome environments validate the promising and robust performance of the proposed detector.**

***Index Terms*—Classifier, Doppler radar, fall detection, wavelet.**

I. Introduction

HUMAN falls are a main cause to morbidity among older adults (aged 65 years and older) [1]. Preventing falls and detecting when they occur are important for elder care. Timely detection of falls enables immediate assistance by caregiver and minimizes the negative consequences of falls [2].

Apart from the clinical techniques, less expensive personal fall detection devices are becoming available in the commercial market. These devices can be broadly classified as wearable [3]–[7] and nonwearable [8]–[17]. Nonwearable devices are often nonobtrusive and more acceptable to the users with better comfort. A commonly found nonobtrusive fall detection device is the video camera [8]–[12], where image processing techniques can isolate and detect falls. However, visual-based systems cannot function under low-lighting or occlusion environments. Another is the microphone array that utilizes the acoustic signal generated from the impact with the floor for fall detection [13]–[15]. Acoustic devices have the shortcoming of requiring relatively quiet environments with little multipath reflections. Both the visual and audio systems can work and complement with each other for inhome fall detection to provide reliable results. Both cannot be used; however, in the bathroom area where statistics have shown to be challenging for fall detection [18]. Having video camera in the bathroom is obviously not preferred. Also, the small dimension of a bathroom would create too many multipath reflections to render the proper performance of an acoustic system, not to mention the strong acoustic interferences from water flowing. In this paper, we explore a relatively new approach based on motion sensing by a Doppler range control radar (RCR) that would fill the need for fall detection, especially in the bathroom.

A human fall generates motion that creates frequency change between the sent and received signals of a Doppler radar. Analyzing the radar signal carefully can detect human falls [19], [20]. A Doppler radar fall detection system separates itself from the image-based and the acoustic-based system in that it can operate in low-lighting and highly noisy environments. In addition, the radar detection system can address the privacy concerns, which are particularly crucial in the bathrooms or bedrooms.

One challenge for radar fall detection is that the radar will generate responses not only from human falls but also from other human or nonhuman motions. Signal processing is an indispensable component to screen out the nonfall activities for improving processing efficiency and increasing detection accuracy. Mel-frequency cepstrum coefficients (MFCC) have been proposed previously for radar fall detection [19]. MFCC is known to have excellent features for speech recognition [21]. However, the rationale of using it in radar is not clear. Extensive evaluations under practical inhome environments indicate the performance of MFCC is not adequate and generates an exceeding number of false alarms in radar fall detection.

This paper investigates another signal processing technique called Wavelet transform (WT) [22] for radar fall activity detection. WT is a very effective method to analyze and extract the characteristics of a signal that has nonstationary behaviors [23]–[25] such as the radar fall signal. Indeed, WT has been proposed recently by many researchers to process biomedical signals such as electrocardiographic [26] data and heart sound [23], [24] with numerous successes.

A fundamental question of using WT for radar fall detection is the choice of the wavelet function. WT uses the dilated and translated versions of a wavelet function to form bases for signal decomposition. In this paper, we examine over 100 wavelet functions and identify the ones that are suitable for fall detection.

The proposed radar fall detection is a two-stage processing: prescreening and classification. The radar data comes in continuously and the first stage applies the WT coefficients at a

Manuscript received August 5, 2014; revised October 24, 2014; accepted October 27, 2014. Date of publication November 4, 2014; date of current version February 16, 2015. This work was supported by the Agency for Healthcare Research and Quality under Grant R01HS018477.

B. Y. Su and M. Skubic are with the ECE Department, University of Missouri, Columbia, MO 65211 USA (e-mail: bsdg6@mail.missouri.edu; SkubicM@missouri.edu).

K. C. Ho is with the ECE Department, University of Missouri, Columbia, MO 65211 USA (e-mail: HoD@missouri.edu).

M. Rantz is with the Sinclair School of Nursing, University of Missouri, Columbia, MO 65211 USA (e-mail: RantzM@missouri.edu).

Color versions of one or more of the figures in this paper are available online at http://ieeexplore.ieee.org.

Digital Object Identifier 10.1109/TBME.2014.2367038

particular scale to locate an instance when potential fall activities may have occurred. The second stage forms feature vector using the WT coefficients at many scales over the time region identified and performs fall versus nonfall classification through a trained classifier. A detection would trigger an alert to a caregiver.

The contributions of this paper includes the introduction of using the WT for radar fall detection, the developments of the WT prescreener and classifier that perform significantly better than the previous methods, and the performance evaluations of the proposed radar fall activity detector with a wide variety of fall types and the actual fall data from an elderly person.

Closely related to our study, Gadde *et al.* [27] recently proposed the use of wavelet processing for fall detection as well, where three features are extracted from the continuous WT of a radar signal for fall versus sit/stand classification using the Mahalanobis distance. The investigation here uses the discrete WT at dyadic scales instead which would reduce the complexity [28]. Gadde *et al.* [27] chooses the Morlet wavelet, and we conduct a study to determine the wavelet function that yields the best performance for the fall detection problem. The features of the proposed classifier are different from those in [27]. We are able to advance the performance as illustrated in Section VI, through extensive evaluations on data measurements from laboratory and inhome environments containing realistic and actual human falls of many kinds. In addition, we establish the use of the wavelet coefficients at a certain scale for prescreening to identify time segments for fall versus nonfall classification. Gadde *et al.* [27] focuses on classification only and applies an energy detector for prescreening, which yields larger amounts of false alarms for the classifier to handle.

This paper is organized as follows. Section II gives a brief background on Doppler radar. Section III provides the rationale of using the WT for radar fall activity detection. Section IV elaborates the details of the proposed fall activity detector using the WT. Section V describes the data measurements for performance evaluations, and Section VI provides the results and comparisons. Finally, we draw conclusions in Section VII.

II. Doppler Radar

Doppler radar is a device that produces responses resulted from the Doppler effect caused by the motion of an object along the radar-object direction [29]. A Doppler radar sends out gated sinusoids (modulated rectangular pulses) at radio frequencies and measures the echo reflected by a moving object. The Doppler effect creates frequency difference between the sent and received signals and the radar output contains harmonics at the frequency change.

The radar used in this study is a commercially available pulse-Doppler RCR [30] which has a price comparable to a webcam. The pulse repetition rate is 10 MHz and the duty cycle is 40%. The carrier frequency f_c is 5.8 GHz. The radar mixes the sent and received signals and applies a low-pass filter to produce the output. The radar output is then digitized at a sampling frequency of 960 Hz.

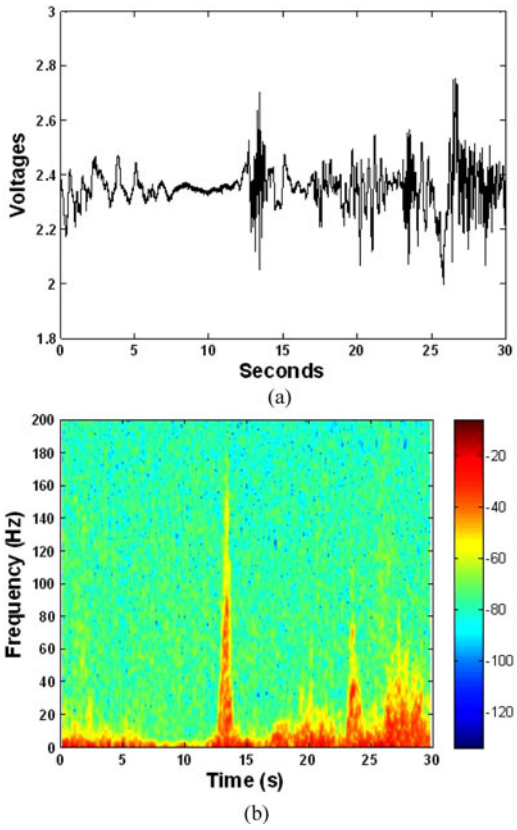

Fig. 1. (a) Waveform of radar output from human fall, the fall is occurred at 14 s. (b) Spectrum of (a).

Fig. 1(a) gives a sample waveform of the radar output containing a human fall, and Fig. 1(b) is its spectrogram. The fall happens at around 14 s. Due to the dynamics of the fall, a higher frequency response appears at the beginning followed by lower frequency content. A human fall typically reaches to about $v = 5$ m/s before hitting the ground. Using the Doppler frequency formula [31]

$$\Delta f_{\max} = \frac{2v}{c} f_c \tag{1}$$

where $c = 3 \times 10^8$ m/s is the light speed. We expect the fall signal covers a frequency range from 0 up to the maximum Doppler shift of about $\Delta f_{\max} = 200$ Hz. The prediction is consistent with the spectrogram shown in Fig. 1(b).

Although we use this particular radar for investigation, the WT technique for radar fall detection is general and can be applied to other Doppler radar with straightforward adjustments.

III. Wavelet Transform

The Fourier transform (FT) is typically used when analyzing data in the frequency domain. One fundamental assumption of the FT is that the data are stationary (or at least wide-sense stationary) with time invariant statistical properties. It divides the frequency range occupied by the data into bins of equal size to examine the frequency content within. For biomedical applications, most of the signals encountered are nonstationary,

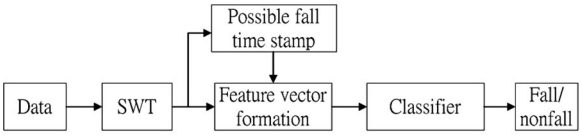

Fig. 2. Data processing blocks for fall activity detection.

and they contain high-frequency components of short bursts and low frequency content of long durations. The FT is not sufficient and not suitable to analyze these kinds of signals, and the WT has been developed to better examine these kinds of nonstationary signals [22].

A human fall typically starts with a quick movement of falling down, followed by a slow motion of lying on the floor. A Doppler radar captures the entire fall activity and produces similar dynamic characteristics of short duration of high frequencies and long period of low frequencies in the output. This kind of signal behavior makes the WT a good choice for data analysis and feature extractions for Doppler radar.

The continuous WT of a signal $x(t)$ is defined as [22]

$$X(\tau, a) = \frac{1}{\sqrt{a}} \int x(t) f^* \left(\frac{t-\tau}{a} \right) dt \tag{2}$$

where f^* is the wavelet function. a is the scale factor, and it is positive for practical applications. The wavelet is dilated when $a > 1$ and contracted when $a < 1$. τ is the translation and $1/\sqrt{a}$ is the energy normalization factor. Different choices of the wavelet function will yield different WT.

The data are in sampled form in practice. By limiting the scale a to be dyadic, the WT has a very efficient implementation by using a pair of filters, one high-pass and the other low-pass, to represent the wavelet function [22]. The resulting WT is often termed as Discrete Stationary Wavelet Transform (SWT) [32] in the literature. SWT is an online processing that transforms the incoming data sequentially through successive applications of the filters. The SWT is redundant in the sense that it will generate the same number of samples in each dyadic scale as in the original data.

It is imperative to determine which wavelet function can provide better performance in extracting the fall information and suppressing the nonfall activities. We shall use the area under the receiver operating characteristic (ROC) [33] curve to select the wavelets. The details will be deferred to Section IV.

IV. Algorithm

Fig. 2 shows the block diagram of the proposed WT fall activity detector. The data first passes through SWT to generate the wavelet coefficients at a number of dyadic scales. The coefficients at a particular scale, scale 4 in our case, will be used to identify the possible time location at which fall activity may have occurred. The SWT coefficients of other scales around the identified time location will form a feature vector, which is used by a classifier to perform fall versus nonfall classification. The details of the prescreening stage to locate the fall occurrence and the classification stage to detect the fall behavior are elaborated in details below.

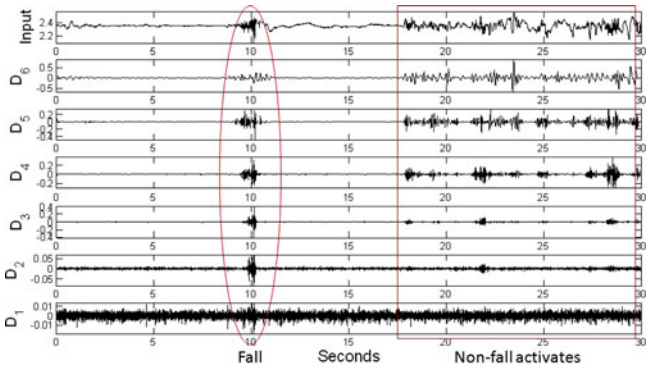

Fig. 3. Multilevel wavelet decomposition of Doppler radar signal.

A. Prescreening Stage

Prescreening should maintain 100% true positives, while seeking to minimize as many false positives as possible. To make a balance between efficiency and complexity, we use only a single scale for processing in this stage.

Through theoretical study and validation by experimental results, scale 4 is the best scale for prescreening. At the sampling rate of 960 Hz, scale 4 corresponds to a frequency range of about 120 to 240 Hz [22]. Using (1), we get the speed range of 3 to 6 $\mathrm{m/s}$, which is what we expect at the early stage of a fall before hitting the ground.

Fig. 3 is an example of the wavelet decomposition over a data segment shown at the top, which contains a fall around 10 s and several nonfall activities between 17.5 and 30 s. The SWT outputs at scales 2^i, denoted by $D_i(n), i = 1, 2, \ldots, 6$ are depicted below the data segment, where the wavelet function is the reverse biorthogonal 3.3 (rbio3.3) [34]. Note that they do not share a common range in the y-axis. Although the WT coefficients over the fall are becoming larger as the scale increases from 2 to 64, the coefficients $D_2(n)$ (scale 4) has the largest fall to nonfall distinction. This observation is consistent with the expectation from theory. We, therefore, use $D_2(n)$ for prescreening.

The fall confidence value for prescreening is the short-time energy of $D_2(n)$ over a moving window to average out variations. The window is Hamming; the window size is 0.5 s and the amount of overlap is 50%. Hence, the location resolution of a fall is 0.25 s. In essence, the prescreener detection value at frame j is

$$C(j) = \sum_{l=1}^{N} \left(w(l)(D_2(l + j(N/2))) \right)^2 . \tag{3}$$

where $w(l)$ represents the Hamming window and, $N = 480$ corresponds to the number of samples in 0.5 s.

A typical fall lasts about 2 s, and a detection is declared if several consecutive $C(j)$ values over a 2 s window exceed the threshold. The frame that has the maximum prescreener

value among the neighboring frames will be assigned as the potential fall location and it will be denoted by j_p. We use a 0.5 s frame instead of 2 s for computing the prescreener value to provide a more accurate time location of a possible fall event to the classifier. A 0.5 s window size also allows us to reuse the prescreener values in the classifier.

Wavelet Selection: It is essential to determine which wavelet function is more suitable for fall detection. We shall use the detection performance curve which is the detection rate versus the number of false alarms, and calculate the area under the curve as an index to evaluate the detection performance from different wavelet functions. When computing the area, the *y*-axis is the detection rate from 0 to 1 and the *x*-axis is from 0 to the largest number of false alarms for reaching 100% detection over the wavelet functions tested. The better wavelet function for fall detection is the one that gives largest area.

In generating the detection performance curve, the detection rate and the number of false alarms are obtained using the prescreening detection statistic $C(j)$ after alarm merging by stepping down the detection threshold. A typical fall is not more than 2 s long, and we have one detection value for every 0.25 s. Contiguous detections up to a maximum of eight frames are merged together with the largest among them as the merged confidence. Noncontiguous detections are counted as separate even if they are within eight frames.

The ROC is produced using the dataset collected in the lab as will be described in Section V. We defer the details of the results for optimum wavelet selection to Section VI.

B. Time–Frequency Features

The alarms from the prescreening stage detects any motion at 3 to 6 m/s. This is a characteristic for a fall. Other activities such as sitting down rapidly on a chair or standing up quickly, however, would create similar motion at the velocity range and result in strong detection. Most importantly, the dynamic behavior of a fall that gives rise to the variations in the frequency content during a fall has not been explored. The classification stage focuses on extracting the time–frequency features from the WT to improve the fall detection performance.

The feature vector for classification is the concatenation of the features from several frames centered at the fall location j_p identified by the prescreener. For a given frame j, we compute the energy of the WT coefficients within after windowing:

$$E_i(j) = \sum_{l=1}^{N} \left(w(l)\, D_i(\, l + j(N/2)\,) \right)^2 \tag{4}$$

where $i = 1, 2, \ldots, 6$, $w(l)$ is the Hamming window, $D_i(n)$ is the WT coefficients at scale 2^i, and $N = 480$ is the window size in samples corresponding to 0.5 s. The values $E_i(j)$ characterize the time–frequency content represented by six dyadic scales in frame j. The window advances 0.25 s. (240 samples) to yield the time–frequency content for the next frame.

The identified fall location from the prescreener is at the early stage of a fall before hitting the ground. We, therefore, collect the time–frequency content over the time range from 1 s before the fall location to 1.5 s after for classification. Considering a typical fall of 2 s long, the extra 0.5 s provides a margin for capturing the fall. This duration, under a frame size of 0.5 s and 50% overlap, translates to four frames before and four frames after the frame j_p.

The main purpose of the classification stage is to exploit the changes in the time–frequency content during a fall to achieve better detection performance. Rather than using $E_i(j)$, we remove the energy factor in each scale through normalization with the WT energy at that scale over the fall duration

$$\tilde{E}_i(j) = \frac{E_i(j)}{\sum_{m=-M}^{M} E_i(j_p + m)} \tag{5}$$

where $j = j_p - M, j_p - M + 1, \ldots, j_p + M$, and $M = 4$. The features of frame j are

$$\mathbf{v}(j) = [\, \tilde{E}_1(j),\, \tilde{E}_2(j),\, \ldots,\, \tilde{E}_6(j)\,]\,. \tag{6}$$

The overall feature vector for classification is

$$\mathbf{v} = \left[\, \mathbf{v}_{j_p - M},\ \mathbf{v}_{j_p - M + 1},\ \ldots, \mathbf{v}_{j_p + M}\, \right]\,. \tag{7}$$

The feature vector contains six normalized energies per frame over nine frames, giving a length of 54.

C. Classifier

We use the nearest neighbor (NN) classifier with the feature vector $\mathbf{v}$. NN is the special case of the k-NN classifier having k equal to 1. Given a test sample $\mathbf{v}_{\rm test}$, we obtain the l_1 norm [35] between $\mathbf{v}_{\rm test}$ and the nearest training sample of falls $\mathbf{v}_{\rm train,fall}$

$$\mathrm{dist}_{\rm fall} = |\mathbf{v}_{\rm test} - \mathbf{v}_{\rm train,fall}|\,. \tag{8}$$

The l_1 norm with respect to the closest nonfall training sample is obtained similarly

$$\mathrm{dist}_{\rm nonfall} = |\mathbf{v}_{\rm test} - \mathbf{v}_{\rm train,nonfall}|\,. \tag{9}$$

The statistic for fall detection is

$$\mathrm{conf} = \mathrm{dist}_{\rm nonfall} - \mathrm{dist}_{\rm fall}\,. \tag{10}$$

Varying the detection threshold will trace out a detection performance curve.

Although simple, NN provides reasonably good results due to the effectiveness of the time–frequency features from the WT. We have tested other classifiers such as SVM with linear and Gaussian kernel functions and the results are not as good as NN.

V. Data Description

The Doppler radar used in the experimental study is the GE Security PrecisionLine RCR-50 [30] whose characteristics have been described in Section II. The radar data acquisition unit is DATAQ DI710 [36] at 960 Hz sampling. The data collections from human subjects have been approved by the Institutional Review Board at the University of Missouri.

The performance evaluation of the proposed fall detection system contains three datasets. The first dataset D0 was collected in 2011, under a laboratory that simulates a home environment. The second dataset D1 was acquired in 2013, in the bathrooms of several senior residence apartments at TigerPlace [37]. The third dataset D2 was taken also in a senior residence apartment

TABLE I
DESCRIPTION OF D0

Fall	times	Acted Nonfall	times
Loose balance-Forward	5	Walk	486
Loose balance-Backward	5	Kick	107
Loose balance-Left	5	Clapping strongly	107
Loose balance-Right	5	Bend over	4
Loss consciousness-Forward	5		
Loss consciousness-Backward	5		
Loss consciousness-Left	5		
Loss consciousness-Right	5		
Loss consciousness-Straight down	5		
Trip and fall-Forward	5		
Trip and fall-Sideways	5		
Slip and fall-Forward	5		
Slip and fall-Sideways	5		
Slip and fall-Backward	5		
Reach-fall (chair)-Forward	5		
Reach-fall (chair)-Left	5		
Reach-fall (chair)-Right	5		
Reach-fall (chair)-Sliding forward	5		
Reach-fall (chair)-Sliding backward	5		
Couch fall-Upper body first	5		
Couch fall-Hip first	5		

TABLE II
STUNT ACTOR INFORMATION OF D0

Subject	Gender	Age	Height (cm)	Weight (kg)
Stunt actor A	female	32	160	61
Stunt actor B	female	46	163	53
Stunt actor C	male	30	173	77

at TigerPlace in 2013, but in the living room (not the bathroom) with actual falls from an elderly resident. The data were recorded continuously in time as the detection system operates in clinical practice and we did not manually isolate out the fall and nonfall segments.

For D0, the dimension of the simulated living room was 9 m $\times$ 8.2 m $\times$ 3 m (L $\times$ W $\times$ H). The radar was mounted at the ceiling center pointing downward. The dataset contains 21 kinds of falls from a combination of various fall types and directions as tabulated in Table I. Each was performed five times from professional stunt actors, whose statistics are summarized in Table II, to strongly resemble the falls of elders after training by nursing staff [38]. The dataset has eight kinds of acted nonfalls that are typical daily activities. The total number of falls is 105 and that of acted nonfalls is 704. The total length of D0 is 145 min. The data were collected and processed continually.

In addition to the intentional nonfalls described in Table I, there are many unintentional nonfall activities during the data collection such as warming up, actively moving right before or after falls, sitting down on a chair, reclining on a sofa, and standing up after performing each fall. These activities create an additional 286 nonfalls. Furthermore, when preparing the experiment, repositioning the sofa, opening the door, moving the fall protection pad, and pulling the chair will also generate many nonfall activities.

TABLE III
STUNT ACTOR INFORMATION OF D1

Subject	Gender	Age	Height (cm)	Weight (kg)
Stunt actor A	female	34	160	60.8

TABLE IV
DESCRIPTION OF FALLS IN D1

Fall	Jan	Feb	Mar	Apr	May
Loose balance-Forward	0	1	2	2	6
Loose balance-Backward	1	0	2	0	6
Loose balance-Left	1	1	0	0	6
Loose balance-Right	1	1	2	0	6
Loss consciousness-Forward	0	1	2	0	0
Loss consciousness-Backward	1	0	2	0	0
Loss consciousness-Left	1	1	0	0	0
Loss consciousness-Right	1	0	2	0	0
Loss consciousness-Straight down	0	1	0	2	0
Trip and fall-Forward	1	0	0	0	0
Trip and fall-Sideways	1	1	0	0	0
Slip and fall-Forward	1	1	2	0	0
Slip and fall-Sideways	0	1	2	2	0
Slip and fall-Backward	0	0	2	2	0
Reach-fall (chair)-Forward	0	0	2	0	0
Reach-fall (chair)-Left	1	0	0	0	0
Reach-fall (chair)-Right	1	1	0	0	0
Reach-fall (chair)-Sliding forward	1	1	2	0	0
Reach-fall (chair)-Sliding backward	0	1	2	2	0

In dataset D1, the stunt actor A, the same as the one in D0 with information given in Table III, performed falls and nonfalls at three different bathrooms at TigerPlace apartment over a period of five months. Two bathrooms have dimensions 2.6 m $\times$ 2.4 m $\times$ 2.7 m and one has 2.3 m $\times$ 2.3 m $\times$ 2.7 m. The radar was mounted in the middle of the bathrooms, above in the attic. The dataset D1 has 211 min in total from the collections over five different months. The kinds of falls in D1 (see Table IV) are the same as in D0 except the last two. Fourteen types of nonfall activities are specifically performed to emulate real-life scenarios as follows. The counts for them in the five months are listed in Table V.

1) Bend at the knees and stoop to a squatting position on the floor, from a standing position.
2) Bend down and kneel on the floor, from a standing position.
3) Bend down and kneel on the floor, wait for 2 s, then lie down on the floor, from a standing position.
4) Bend down to plug an appliance into an electrical outlet close to the floor, from a standing position.
5) Squat to tie a shoe, from a standing position.
6) Sit on the floor with the legs tucked under the body, from a standing position.
7) Sit on the floor with the legs extended from the body, from a standing position.

TABLE V
DESCRIPTION OF NONFALLS IN D1

Nonfall Type	Jan	Feb	Mar	Apr	May
1	0	0	0	0	2
2	1	0	0	0	2
3	1	1	0	0	2
4	1	1	2	2	0
5	0	1	2	2	0
6	0	0	2	0	0
7	0	0	0	0	0
8	1	2	2	2	4
9	2	1	4	0	2
10	0	1	2	2	2
11	1	0	2	0	2
12	1	1	0	0	2
13	1	1	2	0	0
14	3	3	6	2	6

TABLE VI
RESIDENT'S (IN TIGERPLACE) INFORMATION OF D2

Subject	Gender	Age	Height (cm)	Weight (kg)
1	female	75	160	63.5

8) Perform three sit-ups and some stretches of upper and lower extremities, from a lying position on the floor.
9) Slowly rise to a half kneeling position, then rise to a standing position, from a lying position on the floor.
10) Appear to trip but will regain balance and continue walking, from a walking position.
11) Walk forward for 3 s and then stop suddenly, from a standing position.
12) Walk forward for 3 s and then stop suddenly and turn around, from a standing position.
13) Walk to a stationary chair and sit on it, from a standing position.
14) Bend over to pick up a book on the floor, from a sitting position in a chair.

As in D0, D1 also contains those unintentional nonfall activities, which are not listed in Table V.

The dataset D2 is real life data acquired during the daily living of an elderly resident whose statistics are summarized in Table VI. The radar was placed above the middle of the living room (4.4 m $\times$ 6.4 m $\times$ 2.7 m) at the attic in a TigerPlace apartment. The dataset is ten days long containing 13 real falls from the resident. At least one fall occurred in each day and the normal daily activities contribute to nonfalls. The subject has a cat that has a weight of 3.8 Kg. The staff of the TigerPlace came inside the apartment every day to help the subject and other people visited during a day. The data portions with staff or visitors present are removed, for the purpose to assess performance of the radar fall detection system under natural behavior of the resident alone. Indeed, automated fall detection is not urgent when others are present.

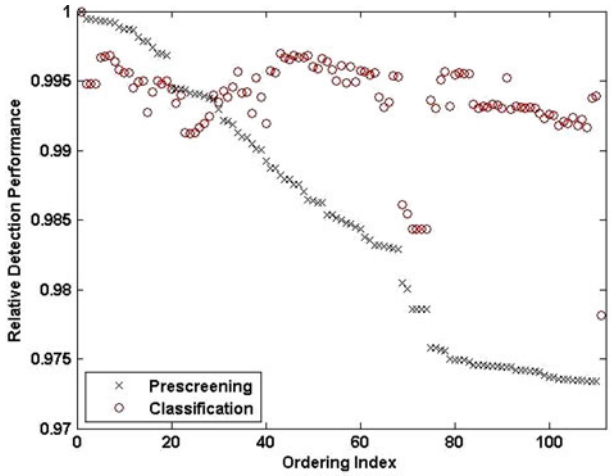

Fig. 4. Relative detection performance from different wavelet functions.

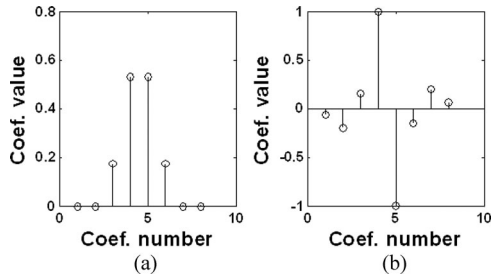

Fig. 5. Wavelet function rbio3.3 represented by a pair of filters in decomposition. (a) Decomposition low-pass filter coefficients. (b) Decomposition high-pass filter coefficients.

VI. EXPERIMENTAL RESULTS

A. Wavelet Selection

We shall use the detection performance from the prescreener on D0 to evaluate the performance of different wavelet functions for fall detection.

We test 111 commonly used wavelet functions for evaluations [28], [34]:

1) Daubechies (db) 1 $\sim$ 45;
2) biorthogonal (bior) and reverse biorthogonal (rbio) series (1.1, 1.3, 1.5, 2.2, 2.4, 2.6, 2.8, 3.1, 3.3, 3.5, 3.7, 3.9, 4.4, 5.5, 6.8);
3) coiflets (coif) 1 $\sim$ 5;
4) discrete approximation of Meyer wavelet (dmey);
5) symlets (sym) 1 $\sim$ 30.

The areas under the detection curves from the wavelet functions are sorted in descending order and the results after normalizing them with the largest area are shown in Fig. 4 using cross symbols. The best five wavelets are "rbio3.3," "db3," "sym3," "rbio1.3," and "bior2.2." Fig. 5 shows the low-pass and the high-pass filter representation of "rbio3.3." The worst one is "rbio3.1" with a normalized area of 0.85.

To support the use of the second level of wavelet decomposition ($a = 4$) for prescreening, Fig. 6 shows the ROC curves from different scales of the wavelet rbio3.3. It confirms that

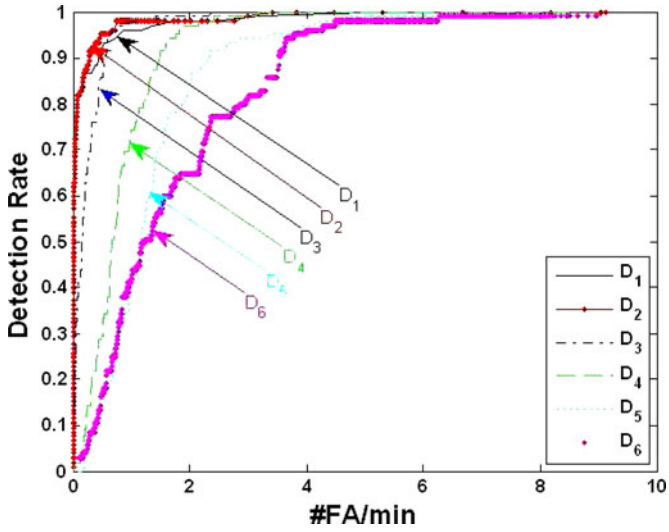

Fig. 6. Prescreening ROCs of D0 using the wavelet coefficients from rbio3.3 at different scales.

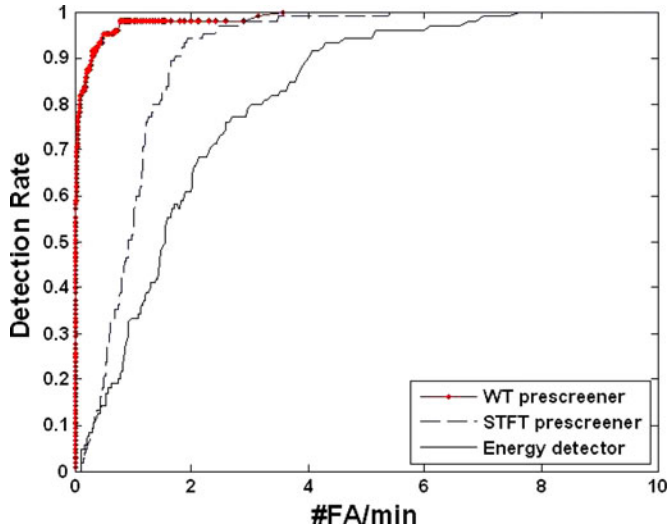

Fig. 7. Prescreener detection performance for D0.

the wavelet coefficients at scale 4 provide better detection than those from other scales.

A better wavelet function for prescreening would yield smaller number of nonfalls for classification. It would reduce the effort of a classifier and provide better detection accuracy after classification as well.

We next examine the classification performance of different wavelet functions, at the detection locations identified by the prescreener using its best wavelet function "rbio3.3." The areas under the detection curves relative to the largest are shown in Fig. 4 using circle symbols. The top five wavelets for the classification stage are "rbio3.3," "coif4," "db10," "bior2.6," and "db11." It is interesting that "rbio3.3" gives the best performance for both prescreening and classification.

For the results presented in the rest of this section, we use the "rbio3.3" in both the prescreening and classification stages.

B. Performance Evaluation

1) Prescreening: For reference purpose, we generate the performance of the energy detector from the input signal as follows:

$$X_{\text{energy}}(j) = \frac{1}{M}\sum_{n=1}^{M}(w(n))((x(n+j(M/2)))^2) \qquad (11)$$

where $X_{\text{energy}}(j)$ represents the signal energy in frame j, and $x(n)$ is the radar data samples. The index n denotes the sample number within the segment, and M corresponds to the number of samples with the 2 s window size. $w(n)$ is the Hamming window function. We shall use $X_{\text{energy}}(i)$ to create the energy detector ROC curve.

In addition to the energy detector, we also generated the results from the detector developed in [19], which is based on the short-time Fourier transform (STFT). Figs. 7 and 8 compare the fall detection performance from the three prescreeners for datasets D0 and D1. As expected, both the proposed WT

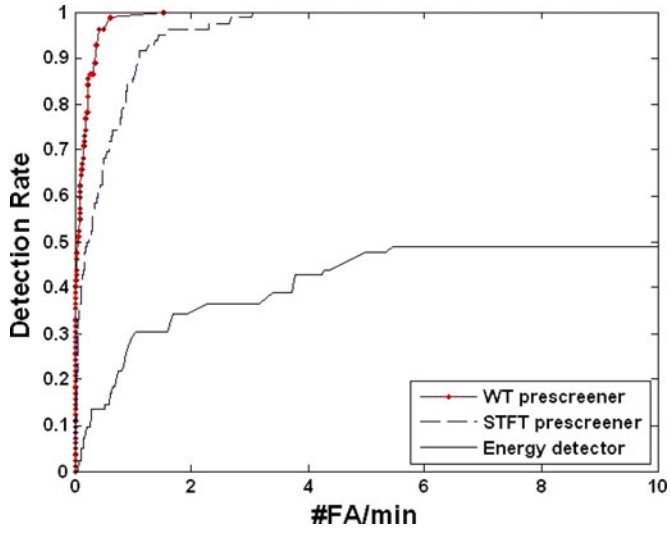

Fig. 8. Prescreener detection performance for D1.

prescreener and the STFT prescreener perform better than the energy detector; the difference is particularly obvious in D1. The proposed WT prescreener is much more effective than the STFT prescreener. At 95% detection rate, the reduction in the number of false alarms is almost by a factor of 3.

2) Classification: We shall use the proposed prescreener to locate the possible fall activities and then apply a classifier to improve the performance. We shall compare the proposed wavelet features with the MFCC features developed in [19]. For a fair comparison, both features are used to train the same kind of classifier, which is the NN, for classification. We also implemented the classification method from [27] that is based on three time-scale (TS) features and the Mahalanobis distance. The cross validation uses leave one out in the training and testing [39].

Fig. 9 shows the ROC classification performance, in terms of sensitivity versus 1-specificity, for D0. The results from the

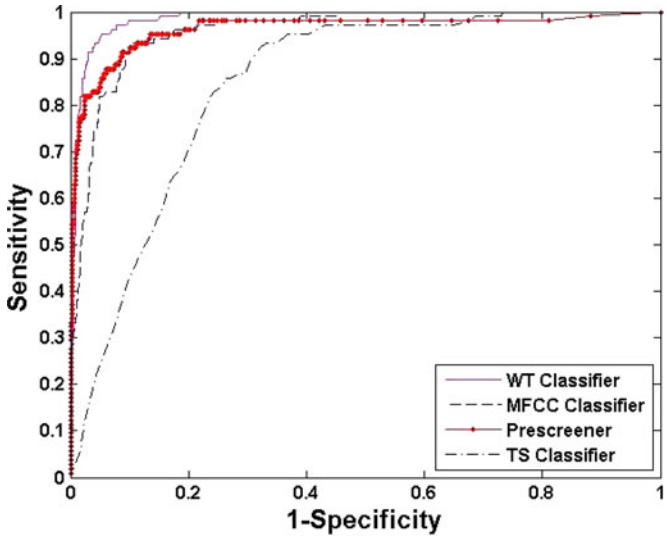

Fig. 9. ROC curves of the proposed and MFCC classifiers for D0.

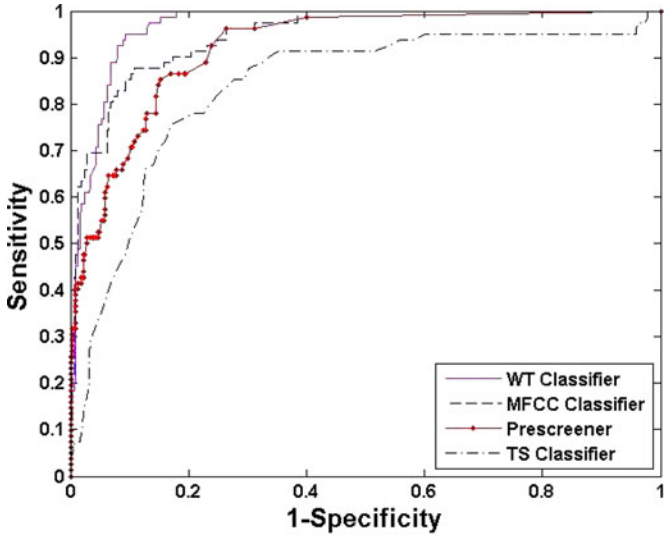

Fig. 10. ROC curves for D1 using leave one out cross validation.

MFCC classifier are worse than the prescreener at the sensitivity below 90% and comparable above. The performance of the TS classifier is also below the prescreener. The proposed WT classifier is able to provide significant performance gain over the prescreener.

To obtain a better understanding, we analyzed the false alarms of the proposed classifier to reach 100% sensitivity. Among these 95 false alarms, 59 are caused by significant human activities such as moving around for preparing and finishing the data collection; 11 from intentional kick actions for time synchronization; 7 from the stunt actors standing up after performing falls; 6 from the warm up actions of the stunt actors; 5 from the stunt actor motion activities right before or after falls; 4 from clapping strongly; 2 from stunt actors bending over; and 1 from a stunt actor lying down on the sofa.

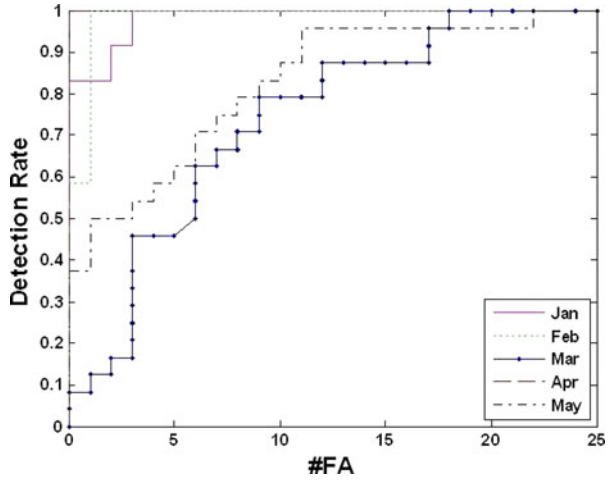

Fig. 11. ROC curves of the proposed classifier for D1 in five different months.

The performance for D1 is shown in Fig. 10. In this dataset, the MFCC classifier has better accuracy than the prescreeener for the sensitivity below 90%. The TS classifier follows the prescreener performance but having a nearly constant decrease in sensitivity at a given specificity. The proposed WT classifier remains the best and outperforms the prescreener considerably. The WT classifier has 58 false alarms to reach 100% detection. Thirty-three false alarms come from significant preparation motions before or after the data collections: 19 from stunt actors standing up after performing falls; 1 from the designed type 3 nonfall activity; 1 from the designed type 4 nonfall activity; 1 from the designed type 13 nonfall activity; and 3 from the designed type 14 nonfall activity.

Fig. 10 is the aggregated results of the data collected over five months from January to May, 2013. Fig. 11 gives the separated performance of the proposed detector for individual months separately. It is interesting to note that detection performance in March and May are particularly worse compared to the others. In the two months, there were extra human activities in preparing the experiments, and the stunt actor was standing up faster than normal after performing the falls. Among the false alarms to reach 100% sensitivity in Fig. 10, 26 out of 33 from activities preparing the experiments, and 14 out of 19 from standing up after falls are from these two months.

In practice, a classifier must be trained beforehand using available data before putting into practical use. The robust performance of the proposed classifier is illustrated in Fig. 12, where we use the lab dataset D0 for training and apply it to the dataset D1 for testing. The proposed classifier has consistent and comparable performance with the cross validation results in Fig. 10, and this is not the case for the MFCC and TS classifiers.

The falls in D0 and D1 are from stunt actors. The apparent large number of false alarms from the proposed classifier to reach 100% detection is caused by nonnatural activities of the stunt actor. Using D2, we are able to assess the performance of the proposed detector for actual falls from an elderly resident in a typical home environment. The proposed prescreener first processes the dataset D2, and the proposed WT or the MFCC

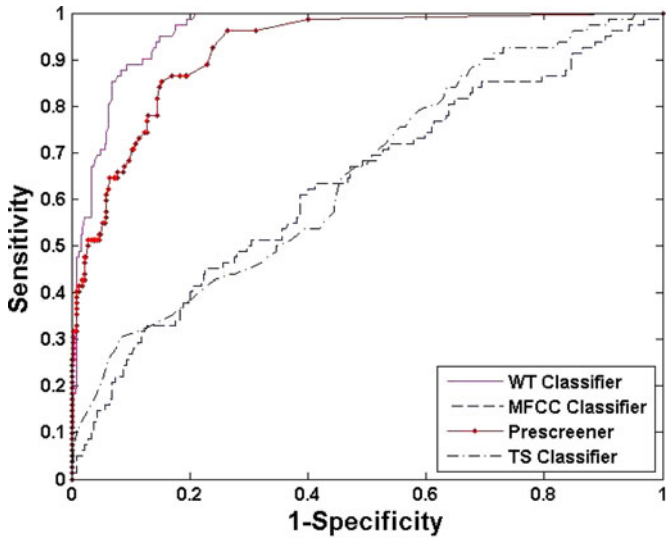

Fig. 12. ROC curves for D1 using D0 as the training data.

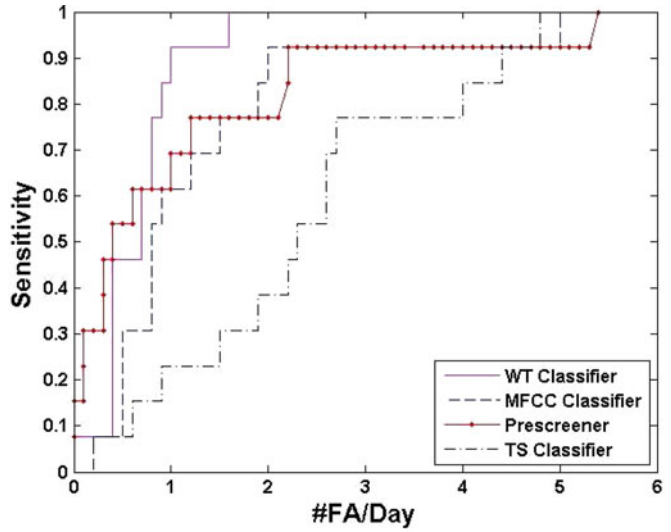

Fig. 13. ROC curves for D2 using D1 as the training data.

classifier operates on the declared locations from a prescreener to produce the detection performance. Training uses dataset D1, where the data from March and May are excluded due to their abnormal behavior.

Fig. 13 illustrates the results. The MFCC classifier produces worst results than the prescreener, which is consistent with the previous observations from Fig. 12. The proposed detector yields promising results. The number of false alarms is much less to reach 100% detection, only 16 over 10 days. The proposed WT fall detector is quite resilient to false positives created by natural daily nonfall activities. Among the 16 false alarms, 11 are from nonhuman activities possibility due to the cat or electromagnetic interference; 1 from random noise with nobody in the living room; 2 from the subject adjusting the height of a chair; 1 from the subject standing up quickly; and 1 from the subject bending over to pick up an object.

TABLE VII
AREA UNDER THE ROC (AUC), SENSITIVITY, SPECIFICITY, AND ACCURACY AT THE OPERATING THRESHOLD

		D0	D1	D2
WT Prescreener	AUC	0.91	0.82	0.71
	Sensitivity	92.3%	86.5%	76.9%
	Specificity	88.9%	80.8%	76.9%
	Accuracy	89.5%	81.9%	77.6%
WT Prescreener and WT Classifier	AUC	0.96	0.92	0.82
	Sensitivity	97.1%	95.1%	92.3%
	Specificity	92.2%	90.7%	81.4%
	Accuracy	93.0%	91.6%	83.5%
WT Prescreener and MFCC Classifier	AUC	0.91	0.85	0.75
	Sensitivity	93.3%	87.8%	92.3%
	Specificity	89.7%	89.1%	62.9%
	Accuracy	90.3%	88.8%	68.6%
WT Prescreener and TS Classifier	AUC	0.76	0.77	0.48
	Sensitivity	85.7%	85.4%	69.2%
	Specificity	71.4%	72.4%	50.0%
	Accuracy	73.8%	75.1%	73.1%

The performance shown in Fig. 13 is for fall detection using radar in the living room of an elderly resident. We expect it represents the lower bound performance for fall detection in the bathroom, since there are more differences between the training and testing data and the living room has more nonfall activities that can cause false positives than the bathroom.

In addition to the ROC curves, Table VII tabulates the performance metrics of the detectors obtained from the three datasets at the operating thresholds [33]. The values shown for D1 are the cross validation results as in Fig. 10. The proposed WT fall detector (WT-based prescreener and classifier) achieves the best and consistent performance. The experimental studies corroborate that the time–frequency features extracted from WT are very effective for fall detection and the proposed fall activity detector has more robust behavior than the previously proposed detector using MFCC features.

The TS classifier [27] also uses wavelet processing and its performance is below expectation. We believe there are two main reasons. First, the three features of the TS classifier are derived from backward falls and sit/stand nonfalls. Datasets D0 and D1 have large varieties of falls and nonfalls performed by professional stunt actors as tabulated in Tables I, IV, and V, and they have different characteristics than just backward falls and sit/stand nonfalls. Second, the radar in [27] was placed 40 in above the floor looking horizontally and our radar was mounted in the ceiling pointing down. A Doppler radar responds to the relative motion along the radar-object direction. The received signals from a ceiling mounted radar and a ground standing radar behave differently. We believe that the TS classifier from [27] would work better when the radar is mounted on a wall looking horizontally.

VII. CONCLUSION

We have developed a reliable detector using Doppler radar measurements for the detection of human falls. The detector is based on WT that explores the time–frequency characteristics of a fall caused by its unique dynamics. The detector has two

stages; the prescreening stage that uses the WT coefficients at a given scale to identify the possible occurrence of a fall, and the classification stage that uses the WT coefficients at several scales over many successive frames to form a feature vector for fall versus nonfall classification. The better wavelet functions to reach higher detection accuracy are "rbio3.3," "db3," "sym3," "rbio1.3," and "bior2.2" for prescreening and "rbio3.3," "coif4," "db10," "bior2.6," "db11" for classification. Evaluations based on the data collected in the lab, in the bathrooms, and in the senior residence apartment validate the promising and robust performance of the proposed WT fall activity detector.

ACKNOWLEDGMENT

The authors would like to thank L. Liu for providing the processing codes of STFT prescreening and MFCC feature extraction from radar signals used in [19].

REFERENCES

[1] S. B. Vyrostek, J. L. Annest, and G. W. Ryan, "Surveillance for fatal and nonfatal injuries—United States, 2001," *MMWR Surveill Summaries*, vol. 53, pp. 1–57, 2004.

[2] F. Bagala, C. Becker, A. Cappello, L. Chiari, K. Aminian, J. M. Hausdorff, W. Zijlstra, and J. Klenk, "Evaluation of accelerometer-based fall detection algorithms on real-world falls," *PLoS ONE*, vol. 7, pp. 1–9, May 2012.

[3] T. Tamrat, M. Griffin, S. Rupcic, S. Kachnowski, T. Taylor, and J. Barfield, "Operationalizing a wireless wearable fall detection sensor for older adults," in *Proc. 6th Int. Conf. PervasiveHealth*, San Diego, CA, USA, May 2012, pp. 297–302.

[4] P. Kumar and P. C. Pandey, "A wearable inertial sensing device for fall detection and motion tracking," in *Proc. IEEE India Annu. Conf.*, Mumbai, India, Dec. 2013, pp. 1–6.

[5] M. Terroso, R. Freitas, J. Gabriel, A. T. Marques, and R. Simoes, "Active assistance for senior healthcare: A wearable system for fall detection," in *Proc. 8th Iberian Conf. Inform. Syst., Technol.*, Lisboa, Portugal, Jun. 2013, pp. 1–6.

[6] W. Bao, Y. Chen, and X. Zeng, "Wearable wireless system with embedded real-time fall detection logic for elderly assisted living applications," in *Proc. IEEE 11th Int. Conf. Solid-State Integr. Circuit Technol.*, Xi'an, China, Oct. 2012, pp. 1–3.

[7] D. Chen, W. Feng, Y. Zhang, X. Li, and T. Wang, "A wearable wireless fall detection system with accelerators," in *Proc. IEEE Int. Conf. Robot. Biomemetics*, Phuket, Thailand, Dec. 2011, pp. 2259–2263.

[8] V. Vaidehi, K. Ganapathy, K. Mohan, A. Aldrin, and K. Nirmal, "Video based automatic fall detection in indoor environment," in *Proc. IEEE Int. Conf. Recent Trends Inform. Technol.*, Chennai, India, Jun. 2011, pp. 1016–1020.

[9] A. Edgcomb and F. Vahid, "Automated fall detection on privacy-enhanced video," in *Proc. IEEE 34th Annu. Int. Conf. Eng. Med. Biol. Soc.*, San Diego, CA, USA, Aug. 2012, pp. 252–255.

[10] V. Vaidehi, K. Ganapathy, K. Mohan, A. Aldrin, and K. Nirmal, "Video based automatic fall detection in indoor environment," in *Proc. IEEE Int. Conf. Recent Trends Inform. Technol.*, Chennai, Tamil Nadu, India, Jun. 2011, pp. 1016–1020.

[11] Y. T. Ngo, H. V. Nguyen, and T. V. Pham, "Study on fall detection based on intelligent video analysis," in *Proc. Int. Conf. Adv. Technol. Commun.*, Hanoi, Vietnam, Oct. 2012, pp. 114–117.

[12] W. Y. Shieh and J. C. Huang, "Speedup the Multi-camera video-surveillance system for elder falling detection," in *Proc. Int. Conf. Embedded Softw, Syst.*, Zhejiang, China, May 2009, pp. 350–355.

[13] Y. Li, Z. Zeng, M. Popescu, and K. C. Ho, "Acoustic fall detection using a circular microphone array," in *Proc. IEEE 32th Annu. Int. Conf. Eng. Med. Biol. Soc.*, Buenos Aires, Argentina, Sep. 2010, pp. 2242–2245.

[14] Y. Li, K. C. Ho, and M. Popescu, "A microphone array system for automatic fall detection," *IEEE Trans. Biomed. Eng.*, vol. 59, no. 5, pp. 1291–1301, May 2012.

[15] O. Gabai and H. Primo, "Acoustic motion capture," U.S. Patent 20 110 009 194, Jan. 13, 2011.

[16] D. Anderson, R. H. Luke, J. M. Keller, M. Skubic, M. Rantz, and M. Aud, "Linguistic summarization of video for fall detection using voxel person and fuzzy logic," *J. Comput. Vision Image Understanding*, vol. 113, pp. 80–89, Jul. 2008.

[17] E. E. Stone and M. Skubic, "Fall detection in homes of older adults using the microsoft kinect," *IEEE J. Biomed. Health Informat.*, to be published.

[18] M. J. Krauss, B. Evanoff, E. Hitcho, K. E. Ngugi, W. C. Dunagan, I. Fischer, S. Birge, S. Johnson, E. Costantinou, and V. J. Fraser, "A case-control study of patient, medication, and care-related risk factors for inpatient falls," *J. Gen. Internal Med.*, vol. 20, pp. 116–122, Feb. 2005.

[19] L. Liu, M. Popescu, M. Rantz, and M. Skubic, "Fall detection using Doppler radar and classifier fusion," in *Proc. IEEE 32th Annu. Int. Eng. Med. Biol. Soc. Conf. BHI*, Hong Kong, Jan. 2012, pp. 180–183.

[20] L. Liu and M. Popescu, "An automatic in-room fall detection system using Doppler radar signatures," submitted for publication *J. Ambient Intell. Smart Environ.*, 2014.

[21] H. Y. Cho and Y. H. Oh, "On the use of channel-attentive MFCC for robust recognition of partially corrupted speech," *IEEE Signal Process. Lett.*, vol. 11, no. 6, pp. 581–584, Jun. 2004.

[22] O. Rioul and M. Vetterli, "Wavelets and signal processing," *IEEE Signal Process. Mag.*, vol. 8, no. 4, pp. 14–38, Oct. 1991.

[23] I. Hossain and Z. Moussavi, "An overview of heart-noise reduction of lung sound using wavelet transform based filter," in *Proc. IEEE 25th Annu. Int. Eng. Med. Biol. Soc. Conf.*, Cancun, Mexico, Sep. 2003, pp. 458–461.

[24] J. J. Lee, S. M. Lee, I. Y. Kim, H. K. Min, and S. H. Hong, "Comparison between short time Fourier and wavelet transform for feature extraction of heart sound," in *Proc. Int. IEEE TENCON Conf.*, Cheju Island, Korea, Dec. 1999, pp. 1547–1550.

[25] M. Yashita and N. Hamada, "Time-frequency masking method using wavelet transform for BSS problem," in *Proc. Int. IEEE TENCON Conf.*, Hong Kong, China, Nov. 2006, pp. 1–4.

[26] L. Brechet, M. F. Lucas, C. Doncarli, and D. Farina, "Compression of biomedical signals with mother wavelet optimization and best-basis wavelet packet selection," *IEEE Trans. Biomed. Eng.*, vol. 54, no. 12, pp. 2186–2192, Dec. 2007.

[27] A. Gadde, M. G. Amin, Y. D. Zhang, and F. Ahmad, "Fall detection and classification based on time-scale radar signal characteristics," *Proc. SPIE*, vol. 9077, May 2014.

[28] S. Mallat, *A Wavelet Tour of Signal Processing.* New York, NY, USA: Academic, 2008.

[29] F. Pfanner, T. Allmendinger, T. Flohr, and M. KachelrieB, "Monitoring respiratory motion using continuous wave Doppler radar in a near field multi antenna approach," in *Proc. Int. IEEE Med. Imag. Conf.*, Anaheim, CA, USA, Oct. 2012, pp. 3575–3581.

[30] Available: http://utcfssecurityproducts.com/

[31] R. W. Ditchburn, *Light*. New York, NY, USA: Dover, 1991, pp. 331–333.

[32] G. P. Nason and B. W. Silverman, "The stationary wavelet transform and some statistical applications," *Lect. Notes Statist.*, vol. 103, pp. 281–299, 1995.

[33] M. H. Zweig and G. Campbell, "Receiver-operating characteristic (ROC) plots: A fundamental evaluation tool in clinical medicine," *Clin. Chem.*, vol. 39, pp. 561–577, 1993.

[34] I. Daubechies, *Ten Lectures on Wavelets*. Philadelphia, PA, USA: SIAM, 1992.

[35] J. W. Williams and Y. Li, "Comparative study of distance functions for nearest neighbors," in *Advanced Techniques in Computing Sciences and Software Engineering*. New York, NY, USA: Springer, 2010, pp. 79–84.

[36] Available: http://www.dataq.com

[37] TigerPlace is an assisted living facility in Columbia, Missouri, USA [Online]. Available: http://eldertech.missouri.edu/

[38] M. J. Rantz, M. A. Aud, G. Alexander, B. J. Wakefield, M. Skubic, R. H. Luke, D. Anderson, and J. M. Keller, "Falls, technology, and stunt actors: New approaches to fall detection and fall risk assessment," *J. Nursing Care Quality*, vol. 23, pp. 195–201, Jul. 2008.

[39] R. Kohavi, "A study of cross-validation and bootstrap for accuracy estimation and model selection," in *Proc. Int. Joint Conf. Artif. Intell.*, Montreal, QC, Canada, Aug. 1995, pp. 1137–1143.

Bo Yu Su (S'14) was born in Taipei, Taiwan. He received the B.S. degree in electrical engineering from National Sun Yat-Sen University, Kaoshiung, Taiwan, in 2002, and the M.S. degree in electrooptical engineering from Tatung University, Taipei, Taiwan, in 2004. He is currently working toward the Ph.D. degree with the Department of Electrical and Computer Engineering, University of Missouri, Columbia, MO, USA.

His current research interests include the Doppler radar and eldercare.

K. C. Ho (M'91–SM'00–F'09) was born in Hong Kong. He received the B.Sc. degree with first class honors in electronics and the Ph.D. degree in electronic engineering, both from the Chinese University of Hong Kong, Shatin, Hong Kong, in 1988 and 1991, respectively.

He was a Research Associate in the Royal Military College of Canada from 1991 to 1994. He joined the Bell-Northern Research, Montreal, QC, Canada in 1995 as a Member of scientific staff. He was a Faculty Member in the Department of Electrical Engineering at the University of Saskatchewan, Saskatoon, Canada, from September 1996 to August 1997. Since September 1997, he has been with the University of Missouri, Columbia, MO, USA, and he is currently a Professor in the Electrical and Computer Engineering Department. He was very active in the ITU standard developments from 1995 to 2012. He is an Inventor of 20 patents in the United States, Europe, Asia, and Canada on geolocation and signal processing for wireless communications. His research interests include sensor array processing, detection and estimation, source localization, wireless communications, and the development of efficient signal processing algorithms for various applications.

Dr. Ho received the Junior Faculty Research Award and the Senior Faculty Research Award from the College of Engineering, University of Missouri. He was the Chair of the Sensor Array and Multichannel Technical Committee in the IEEE Signal Processing Society from 2013 to 2014. He was an Associate Editor of the IEEE TRANSACTIONS ON SIGNAL PROCESSING and the IEEE SIGNAL PROCESSING LETTERS.

Marilyn J. Rantz (M'12) received the Ph.D. degree in nursing from the University of Wisconsin, Milwaukee, WI, USA, in 1992.

She is with the University of Missouri (MU), Columbia, MO, USA, where she is a Faculty Member in the Sinclair School of Nursing and the Department of Family and Community Medicine, MU School of Medicine, where she is currently a Professor. She is also the University Hospital Professor of nursing. She has developed and sustained a research program to improve the quality of care of elderly. Her innovative work in nursing home quality spans nearly 30 years, in practice and as a Leading Researcher, establishes her as a Premier International Expert in quality measurement in nursing homes. She and her multidisciplinary research team has garnered nearly 60 million in funds to support their work measuring effectiveness of nurse care coordination, conduct cutting edge research in long-term care, new delivery models of care, and for technology development to enhance aging in place of community-dwelling elders. Her current research interests include technology to enhance aging in place, long-term care quality measurement, and quality improvement.

Prof. Rantz received both the MU Sinclair School of Nursing Faculty Award for Excellence in Research and the National Gerontological Nursing Association Lifetime Achievement Award in 2005. In 2006, she received the MU Alumni Association Faculty Alumni Award for her outstanding contributions to her profession, the community, and the University of Missouri. She is a Fellow of the American Academy of Nursing.

Marjorie Skubic (S'90–M'91–SM'13) received the Ph.D. degree in computer science from Texas A&M University, College Station, TX, USA, in 1997, where she specialized in distributed telerobotics and robot programming by demonstration.

In 2006, she established the Center for Eldercare and Rehabilitation Technology at the University of Missouri and serves as the Center Director for this interdisciplinary team. The focus of the center's work includes monitoring systems for tracking the physical and cognitive health of elderly residents in their homes, logging sensor data in an accessible database, extracting activity and gait patterns, identifying changes in patterns, and generating alerts for health changes. She is currently a Professor in the Electrical and Computer Engineering Department at the University of Missouri, Columbia, MO, USA, with a joint appointment in computer science. In addition to her academic experience, she has spent 14 years working in industry on real-time applications such as data acquisition and automation. Her current research interests include sensory perception, computational intelligence, spatial referencing interfaces, human–robot interaction, and sensor networks for eldercare.